

Highly efficient mid-infrared 2 μm emission in $\text{Ho}^{3+}/\text{Yb}^{3+}$ -codoped germanate glass

Muzhi Cai,¹ Beier Zhou,¹ Fengchao Wang,¹ Ying Tian,¹ Jiajia Zhou,¹ Shiqing Xu^{1,3} and Junjie Zhang^{1,3}

¹College of Materials Science and Engineering, China Jiliang University, Hangzhou 310018, China

²jjzhang@cjl.u.edu.cn

³shiqingxu@cjl.u.edu.cn

Abstract: This work reports the mid-infrared emission properties around 2 μm in $\text{Ho}^{3+}/\text{Yb}^{3+}$ codoped germanate glasses. The glass not only possesses good chemical durability and good thermal stability but also has high mid-infrared transmittance around 2 μm (90%). In addition, the glass possesses considerably low OH^- content (20.45 ppm) and large spontaneous transition probability (103.38 s^{-1}) corresponding to the $\text{Ho}^{3+} : {}^5\text{I}_7 \rightarrow {}^5\text{I}_8$ transition. Moreover, the measured lifetime of $\text{Ho}^{3+} : {}^5\text{I}_7$ level is as high as 7.68 ms, and the quantum efficiency at 2 μm can reach 79.4%. The energy transfer processes of $\text{Yb}^{3+} : {}^2\text{F}_{5/2}$ level and $\text{Ho}^{3+} : {}^5\text{I}_6$ level were quantitatively analyzed according to the rate equation. Results indicate that the prepared germanate glass is a promising candidate for 2 μm mid-infrared laser materials applications.

©2015 Optical Society of America

OCIS codes: (160.5690) Rare-earth-doped materials; (250.5230) Photoluminescence; (260.2160) Energy transfer; (300.6340) Spectroscopy, infrared.

References and links

1. D. Faucher, M. Bernier, G. Androz, N. Caron, and R. Vallée, “20 W passively cooled single-mode all-fiber laser at 2.8 μm ,” *Opt. Lett.* **36**(7), 1104–1106 (2011).
2. M. C. Pierce, S. D. Jackson, M. R. Dickinson, T. A. King, and P. Sloan, “Laser-tissue interaction with a continuous wave 3- μm fibre laser: Preliminary studies with soft tissue,” *Lasers Surg. Med.* **26**(5), 491–495 (2000).
3. A. Godard, “Infrared (2–12 μm) solid-state laser sources: a review,” *C. R. Phys.* **8**(10), 1100–1128 (2007).
4. T. Hu, D. D. Hudson, B. J. Eggleton, and S. D. Jackson, “A highly-efficient, 2.9 μm Q-switched Ho/Pr co-doped fiber laser,” in *Lasers and Electro-Optics (CLEO), 2012 Conference on* (2012), pp. 1–2.
5. F. Huang, X. Liu, Y. Zhang, L. Hu, and D. Chen, “Enhanced 2.7- and 2.84- μm emissions from diode-pumped $\text{Ho}^{3+}/\text{Er}^{3+}$ -doped fluoride glass,” *Opt. Lett.* **39**(20), 5917–5920 (2014).
6. R. Xu, J. Pan, L. Hu, and J. Zhang, “2.0 μm emission properties and energy transfer processes of $\text{Yb}^{3+}/\text{Ho}^{3+}$ codoped germanate glass,” *J. Appl. Phys.* **108**(4), 043522 (2010).
7. J. J. Pan, R. R. Xu, Y. Tian, K. F. Li, L. L. Hu, and J. J. Zhang, “2.0 μm Emission properties of transparent oxyfluoride glass ceramics doped with Yb^{3+} - Ho^{3+} ions,” *Opt. Mater.* **32**(11), 1451–1455 (2010).
8. G. Bai, L. Tao, K. Li, L. Hu, and Y. H. Tsang, “Enhanced ~2 μm and upconversion emission from Ho–Yb codoped oxyfluoride glass ceramics,” *J. Non-Cryst. Solids* **361**, 13–16 (2013).
9. F. Huang, J. Cheng, X. Liu, L. Hu, and D. Chen, “ $\text{Ho}^{3+}/\text{Er}^{3+}$ doped fluoride glass sensitized by Ce^{3+} pumped by 1550 nm LD for efficient 2.0 μm laser applications,” *Opt. Express* **22**(17), 20924–20935 (2014).
10. A. Hemming, S. Bennetts, N. Simakov, A. Davidson, J. Haub, and A. Carter, “High power operation of cladding pumped holmium-doped silica fibre lasers,” *Opt. Express* **21**(4), 4560–4566 (2013).
11. R. Li, J. Li, L. Shterengas, and S. D. Jackson, “Highly efficient holmium fibre laser diode pumped at 1.94 μm ,” *Electron. Lett.* **47**(19), 1089 (2011).
12. W. Qing, G. Jihong, J. Zhuo, L. Tao, and J. Shibin, “Mode-locked Tm-Ho fiber laser with a Sb-based SESAM,” in *Lasers and Electro-Optics (CLEO), 2011 Conference on* (2011), pp. 1–2.
13. S. D. Jackson, “8.8 W diode-cladding-pumped $\text{Tm}^{3+}/\text{Ho}^{3+}$ -doped fluoride fibre laser,” *Electron. Lett.* **37**(13), 821–822 (2001).
14. F. Fusari, A. A. Lagatsky, G. Jose, S. Calvez, A. Jha, M. D. Dawson, J. A. Gupta, W. Sibbett, and C. T. A. Brown, “Femtosecond mode-locked Tm^{3+} and Tm^{3+} - Ho^{3+} doped 2 μm glass lasers,” *Opt. Express* **18**(21), 22090–22098 (2010).

15. Y. Guo, G. Gao, M. Li, L. Hu, and J. Zhang, "Er³⁺-doped fluoro-tellurite glass: A new choice for 2.7 μm lasers," *Mater. Lett.* **80**, 56–58 (2012).
16. Y. Guo, M. Li, L. Hu, and J. Zhang, "Intense 2.7 μm emission and structural origin in Er³⁺-doped bismuthate (Bi₂O₃-GeO₂-Ga₂O₃-Na₂O) glass," *Opt. Lett.* **37**(2), 268–270 (2012).
17. R.-G. Duan, K.-M. Liang, and S.-R. Gu, "A new criterion for the stability of glasses," *J. Eur. Ceram. Soc.* **18**(8), 1131–1137 (1998).
18. Y. Tian, T. Wei, F. Chen, X. Jing, J. Zhang, and S. Xu, "Fluorescence characteristics and energy transfer of ytterbium-sensitized erbium-doped fluorophosphate glass for amplifier applications," *J. Quant. Spectrosc. Radiat. Transf.* **133**, 311–318 (2014).
19. T. Wei, F. Chen, X. Jing, Y. Tian, F. Wang, and S. Xu, "Mid-infrared fluorescence of Y₂O₃ and Nb₂O₅ modified germanate glasses doped with Er³⁺ pumped by 808nm LD," *Opt. Mater.* **36**(8), 1350–1356 (2014).
20. B. Judd, "Optical Absorption Intensities of Rare-Earth Ions," *Phys. Rev.* **127**(3), 750–761 (1962).
21. G. S. Ofelt, "Intensities of Crystal Spectra of Rare-Earth Ions," *J. Chem. Phys.* **37**(3), 511 (1962).
22. J. Fan, Y. Fan, Y. Yang, D. Chen, L. Calveza, X. Zhang, and L. Zhang, "Spectroscopic properties and energy transfer in Yb³⁺-Ho³⁺ co-doped germanate glass emitting at 2.0 μm," *J. Non-Cryst. Solids* **357**(11-13), 2431–2434 (2011).
23. Y. P. Peng, Y. Guo, J. Zhang, and L. Zhang, "Ho³⁺/Yb³⁺-codoped germanate-tellurite glasses for 2.0 μm emission performance," *Appl. Opt.* **53**(8), 1564–1569 (2014).
24. B. Peng and T. Izumitani, "Optical properties, fluorescence mechanisms and energy transfer in Tm³⁺, Ho³⁺ and Tm³⁺-Ho³⁺ doped near-infrared laser glasses, sensitized by Yb³⁺," *Opt. Mater.* **4**(6), 797–810 (1995).
25. K. Biswas, A. D. Sontakke, R. Sen, and K. Annapurna, "Enhanced 2 μm broad-band emission and NIR to visible frequency up-conversion from Ho³⁺/Yb³⁺ co-doped Bi₂O₃-GeO₂-ZnO glasses," *Spectrochim. Acta A Mol. Biomol. Spectrosc.* **112**, 301–308 (2013).
26. A. Florez, S. L. Oliveira, M. Flórez, L. A. Gómez, and L. A. O. Nunes, "Spectroscopic characterization of Ho³⁺ ion-doped fluoride glass," *J. Alloys Compd.* **418**(1-2), 238–242 (2006).
27. Q. Zhang, G. Chen, G. Zhang, J. Qiu, and D. Chen, "Spectroscopic properties of Ho³⁺/Yb³⁺ codoped lanthanum aluminum germanate glasses with efficient energy transfer," *J. Appl. Phys.* **106**(11), 113102 (2009).
28. L. Tao, Y. H. Tsang, B. Zhou, B. Richards, and A. Jha, "Enhanced 2.0 μm emission and energy transfer in Yb³⁺/Ho³⁺/Ce³⁺ triply doped tellurite glass," *J. Non-Cryst. Solids* **358**(14), 1644–1648 (2012).
29. Y. Tian, R. Xu, L. Zhang, L. Hu, and J. Zhang, "Enhanced effect of Ce³⁺ ions on 2 μm emission and energy transfer properties in Yb³⁺/Ho³⁺ doped fluorophosphate glasses," *J. Appl. Phys.* **109**(8), 083535 (2011).
30. J.-P. Zhang, W.-J. Zhang, J. Yuan, Q. Qian, Q.-Y. Zhang, and B. Dunn, "Enhanced 2.0 μm Emission and Lowered Upconversion Emission in Fluorogermanate Glass-Ceramic Containing LaF₃:Ho³⁺/Yb³⁺ by Codoping Ce³⁺ Ions," *J. Am. Ceram. Soc.* **96**(12), 3836–3841 (2013).
31. J. M. F. van Dijk, "On the nonradiative and radiative decay rates and a modified exponential energy gap law for 4f-4f transitions in rare-earth ions," *J. Chem. Phys.* **78**(9), 5317 (1983).
32. X. Li, Q. Nie, S. Dai, T. Xu, L. Lu, and X. Zhang, "Energy transfer and frequency upconversion in Ho³⁺/Yb³⁺ co-doped bismuth-germanate glasses," *J. Alloys Compd.* **454**(1-2), 510–514 (2008).

1. Introduction

Numerous applications including remote sensing, eye-safe laser radar, atmosphere pollution monitoring, medical surgery and precision guidance, are main driving force behind mid-infrared lasers around 2 μm wavelengths [1–3]. So far, luminescent ions for 2 μm mid-infrared applications have been mainly focused on Tm³⁺ and Ho³⁺ ions owing to the transition of ³F₄→³H₆ at 1.85 μm and ⁵I₇→⁵I₈ at 2.0 μm, respectively. Compared with Tm³⁺ ion, the emission cross section of Ho³⁺ ion is about five times higher than that of Tm³⁺ ion, in addition, the fluorescence lifetime of Ho³⁺ is in favor of Q-switched laser [4–6]. Hence, Ho³⁺-doped glass has become a research hotspot. Ho³⁺ 2.0 μm emission has already been investigated in different kind of glasses and 2.0 μm laser output has been obtained as well [6–9]. Output power of 140 W at 2.1 μm was demonstrated by using a Ho³⁺-doped silica glass fiber laser in 2013 [10]. A maximum slope efficiency of 78% and output power of 516mW at 2.08 μm has been obtained in a Ho³⁺-doped fluoride glass fiber in 2011 [11]. However, Ho³⁺ needs to be pumped around 900 nm or 1100 nm, which is not readily available from existing common commercial laser diodes. One approach to Ho³⁺ lasers is based on materials codoped with other rare earth ion which has strong absorption bands near the wavelength of existing commercial laser diodes. Tm³⁺ and Yb³⁺ ions are more commonly used as the sensitizing ions. A mode-locked Tm³⁺/Ho³⁺-codoped silicate fiber laser with pulse energy of 0.41 nJ and pulse duration of 1.1 ps is reported in 2011 [12]. A maximum output power of 8.8 W at 2.05 μm has been obtained in a Tm³⁺/Ho³⁺-codoped ZBLAN glass fiber [13]. A Tm³⁺/Ho³⁺-codoped

tellurite bulk glass laser with a 26% slope efficiency and a maximum output power of 74 mW at 1012 nm is reported in 2010 [14].

Compare with $\text{Tm}^{3+}/\text{Ho}^{3+}$ -codoped glasses, there are few studies about 2.0 μm emission properties in $\text{Yb}^{3+}/\text{Ho}^{3+}$ codoped glasses. Up to now, host materials mainly focused on silicate glasses and fluoride glasses [6]. Although silicate glass has a good thermal stability and high damage threshold, its high phonon energy which increases nonradiative transition probability limits its luminous quantum efficiency. On the contrast, fluoride has low phonon energy and high rare earth solubility, but its poor chemical durability, mechanical strength and low damage threshold limit its further applications in high power or energy fiber laser systems. In such case, heavy-metal oxide glasses such as germanate glasses and tellurite glasses have become hotspot of research. From the viewpoint of technological application, germanate glass is quite suitable as host material for $\text{Yb}^{3+}/\text{Ho}^{3+}$ 2 μm mid-infrared laser not only because of its superior thermal stability, chemical durability and mechanical strength, but also for the merits of relative low phonon energy and wide infrared transmittance range compared with other oxide glass [6]. In this report, $\text{Ho}^{3+}/\text{Yb}^{3+}$ codoped germanate glasses were prepared and mid-infrared 2.0 μm emission properties were systematically investigated. Moreover, highly efficient 2.0 μm emission with long lifetime were achieved.

2. Experimental procedures

$\text{Yb}^{3+}/\text{Ho}^{3+}$ -codoped germanate glasses were synthesized by conventional melting method, which has the following molar compositions: $(79-x) (\text{GeO}_2 + \text{Ga}_2\text{O}_3) - 20(\text{BaF}_2 + \text{LiF}) - x\text{Ho}_2\text{O}_3 - 1\text{Yb}_2\text{O}_3$ ($x = 0.02, 0.11, 0.17, 0.2$). In addition, Ho^{3+} and Yb^{3+} singly doped sample were also prepared to make a comparison. Samples were synthesized by using high-purity GeO_2 , R_2O_3 , BaF_2 , LiF , Yb_2O_3 and Ho_2O_3 powder. The stoichiometric chemicals were well-mixed and melted at 1400 $^\circ\text{C}$ for 30 min in a covered alumina crucible. Then, the melts were poured onto a preheated steel plate and pressed by another plate for shaping. After annealing at around glass transition temperature, all samples were cut and polished into $10 \times 10 \times 2 \text{ mm}^3$ for further measurement.

Refractive indexes(1.68) of samples were measured by prism minimum deviation method at the wavelength of 1053 nm. The resolution of the instrument was $\pm 0.5 \times 10^{-4}$. The densities($4.4\text{g}/\text{cm}^3$) were tested by Archimedes principle using distilled water as an immersion liquid with error limit of $\pm 0.05\%$. Differential scanning calorimeter (DSC) curve is measured using NETZSCH DTA 404 PC at the heating rate of 15, 20, 25, 30 K/min with maximum error of $\pm 5^\circ\text{C}$. Absorption spectra in the range of 350-2200 nm and transmittance in the range of 1600-3300 nm were recorded with a Perkin-Elmer- Lambda 900UV/VIS/NIR spectrophotometer. Photoluminescence spectra in the ranges of 1800-2200 nm were determined via a combined fluorescence lifetime and steady state spectrometer (FLSP 980) (Edinburgh Co., England), which was detected with a liquid-nitrogen-cooled PbS detector using an 980 nm laser diode (LD) as an excitation source. The 980 nm LD with the same power was also utilized to measure the lifetimes of $\text{Ho}^{3+} {}^5\text{I}_7$ and $\text{Yb}^{3+} {}^2\text{F}_{5/2}$ level. The lifetimes were calculated by fitting a single exponential function to the decay curve with normalized initial intensity. The same experimental conditions for different samples were maintained so as to get comparable results. All the measurements were performed at ambient temperature.

The chemical durability of the present sample was measured as follows. First, the weighed sample (W_1) was placed in distilled water. The glass was then kept in a thermostatic water bath at 95 $^\circ\text{C}$ for 24 h, after which the sample was cooled and dried in a drying box at 80 $^\circ\text{C}$ for 4 h. Finally, the dry sample was weighed again (W_2). The chemical durability of germanate glass sample ($x = 0.17$) was evaluated in terms of the ΔW value, which was calculated as follows [15]:

$$\Delta W = \frac{W_1 - W_2}{W_2} \times 100\% \quad (1)$$

3. Results and discussion

3.1. Chemical durability and Thermal stability

Based on the weight loss experiment, the chemical durability of present glass is evaluated by Eq. (1). The ΔW of present germanate glass is 70 mg/g, this value is approximately half that of ZBLAN glass (151.6 mg/g) [15]. The present glass possesses evidently better chemical durability than ZBLAN and can be stably used in laser applications.

The differential scanning calorimeter (Netzsch) curves were measured for characteristic temperatures (temperature of glass transition T_g , temperature of onset crystallization T_x , and temperature of peak crystallization T_p) as shown in Fig. 1(a). T_g is an important factor for laser glass, a higher one, such as 572 °C in prepared samples than that of fluoride (430°C) [13], gives glass good thermal stability to resist thermal damage at high pumping intensities. Glass optical fibers are currently drawn from preforms, which means that the glass crosses twice the thermal range of instability: first on cooling for preform manufacturing and then on reheating for fiber drawing. Hence, the anti-crystallization ability is a vital requirement for glass. The ΔT ($T_x - T_g$) has been frequently used as a rough indicator of the glass formation ability or glass stability against crystallization, and large ΔT is beneficial to the fiber drawing [14]. The ΔT of the prepared sample is about 178 °C, which is higher than that of bismuthate glass (163°C) [16] and germanate glass (123°C) [6], indicating that the prepared sample has better thermal stability against crystallization.

The activation energy is another indicator of the glass anti-crystallization ability [17]. By the Kissinger model [17], the activation energy E_a under non-isothermal conditions can be written as

$$\ln\left(\frac{T_p^2}{\phi}\right) = \frac{E_a}{RT_p} + \text{constant} \quad (2)$$

in which R is the Universal Gas Constant and ϕ is the heating rate. In order to determine E_a for these glasses, the $\ln(T_p^2/\phi)$ vs $1000/T_p$ curves were calculated, and are shown in Fig. 1(b) for present sample. From the experimental data fit, the activation energy values were determined. The sample activation energy is as high as 350 kJ·mol⁻¹, which is comparable to silicate glass (338.96 kJ·mol⁻¹), indicating the prepared samples actually have good anti-crystallization ability [17].

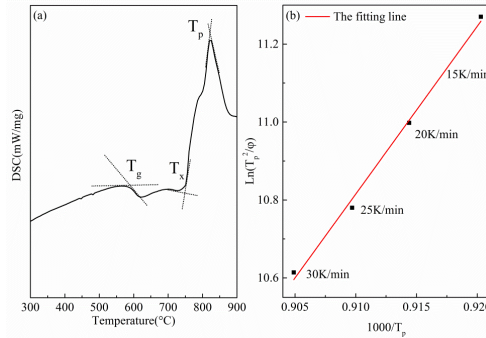


Fig. 1. Fig. 1(a) DSC curve for $x = 0.17$ $\text{Ho}^{3+}/\text{Yb}^{3+}$ -codoped germanate glass with heating rate of 20K/min. (b) $\ln(T_p^2/\phi)$ vs $1000/T_p$ graph for germanate glasses codoped with $\text{Ho}^{3+}/\text{Yb}^{3+}$. The solid line is the fit using the Kissinger method to determine the activation energy.

3.2. Transmittance and FTIR transmittance

Figure 2 presents the transmittance spectrum of the prepared sample ($x = 0.17$) in the wavelength region of 1600-3300 nm. The loss includes the Fresnel reflections, dispersion,

and the absorption of the glass. As can be seen, the transmittance has a slight decline at 2 μm because of the absorption of Ho^{3+} ions. Although the transmittance declined at 3 μm due to the absorption of hydroxyl groups, the transmittance still can reach 89%. In addition, it is known that the contents of OH^- groups have an influence on mid-infrared fluorescence since residual hydroxyl groups in glasses can act as the fluorescence-quenching center. In order to calculate the OH^- content, the Fourier Transform Infrared (FTIR) transmittance spectrum of prepared sample has been also tested as show in the inset of Fig. 2. It is worth noting that the transmittance spectra and FTIR transmittance spectra are different in the wavelength around 3000 nm, because FTIR transmittance spectra is used to illustrate the molecular vibration in glass could not accurately show the transmittance. The OH^- content (in ppm, parts per million) can be evaluated from the infrared transmittance spectrum using the following formula [18]

$$[\text{OH}^-](\text{ppm}) = (1000 / d) \log(T_b / T) \quad (3)$$

where d is the sample thickness in millimeters, T_b is the transmittance at the base line ($\sim 2.5 \mu\text{m}$), and T is the transmission at the maximum absorption of the OH^- band ($\sim 2.9 \mu\text{m}$). It is calculated to be 20.45 ppm in present glass which is evidently lower than fluorophosphate glass (35.5 ppm) [18] and germanate glass (30.6–35.4 ppm) [19]. The result suggests the prepared germanate glass has relatively low OH^- content.

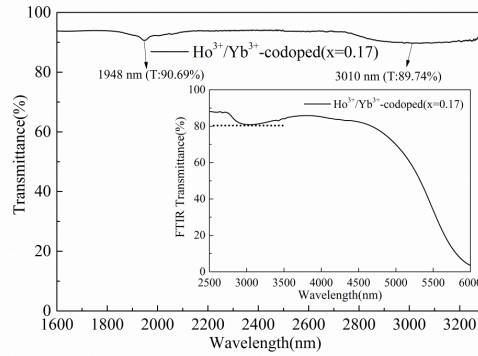


Fig. 2. Transmittance spectra and FTIR transmittance spectra (inset) of $\text{Ho}^{3+}/\text{Yb}^{3+}$ codoped germanate glass ($x = 0.17$).

3.3. Absorption spectra and J-O analysis

The absorption spectra of the Ho^{3+} singly doped, Yb^{3+} singly doped, $\text{Ho}^{3+}/\text{Yb}^{3+}$ -codoped samples at room temperature in the wavelength region of 250–2200 nm are shown in Fig. 3. For Ho^{3+} singly doped sample, absorption bands centered at 1152 nm, 900 nm, 642 nm, 536 nm, 484 nm, 449 nm and 416 nm correspond to the transitions starting from the ground state $^5\text{I}_8$ to excited levels $^5\text{I}_6$, $^5\text{I}_5$, $^5\text{F}_5$, ($^5\text{F}_4 + ^5\text{S}_2$), $^5\text{F}_3$, $^5\text{G}_6$, and $^5\text{G}_5$, respectively. It can be seen that the shape and the peak positions of each transition for Ho^{3+} -doped germanate glass are very similar to those in other Ho^{3+} -doped glasses [6–9]. The intense absorption of the $^2\text{F}_{7/2}$ level to $^2\text{F}_{5/2}$ level of Yb^{3+} is also observed in $\text{Ho}^{3+}/\text{Yb}^{3+}$ codoped sample in the wavelength region of 900–1000 nm, whereas the absorption of the $^5\text{I}_5$ level of Ho^{3+} is too weak to observe, which is indicated that codoping of Yb^{3+} is expected to provide an efficient excitation channel.

Judd–Ofelt theory is widely applied to predict the spectroscopic properties of the f–f transitions of trivalent rare earth ions, which was developed simultaneously and independently by Judd and Ofelt in 1962 [20, 21]. According to the theory, the intensity parameters Ω_t ($t = 2, 4, 6$) were calculated based on the absorption data. The parameter Ω_2 exhibits the dependence on the covalency between rare-earth ions and ligand anions and reflects the asymmetry of the local environment at the Ho^{3+} ion site, while the parameters Ω_4

and Ω_6 relate to the covalency of the medium in which the Ho^{3+} ions are situated. The Ω_4 ($2.92 \times 10^{-6} \text{ cm}^2$) and Ω_6 ($1.4 \times 10^{-6} \text{ cm}^2$) in prepared glass are comparable with those reported germanate glass, while the Ω_2 ($4.55 \times 10^{-6} \text{ cm}^2$) is lower than those of germanate glasses [22, 23]. It is indicated that the prepared sample possesses weaker covalence than other germanate glass. The rms error deviation of intensity parameters is 0.76×10^{-6} , which indicates the validity of the Judd-Ofelt theory for predicting the spectral intensities of Ho^{3+} are reliable calculations. Further calculation about spontaneous radiative transition probability (A_{rad}), fluorescence lifetime (τ_{rad}), and branching ratios (β) of $\text{Ho}^{3+}/\text{Yb}^{3+}$ various transition in prepared glasses are determined. Higher A_{rad} provides a better opportunity to obtain laser actions. The radiative transition probabilities (A) of the $^5\text{I}_7 \rightarrow ^5\text{I}_8$ transition in $x = 0.17$ sample (103.38 s^{-1}) is much higher than that of fluorophosphates glass (90.42 s^{-1}) [24] and germanate glass (88.19 s^{-1}) [23].

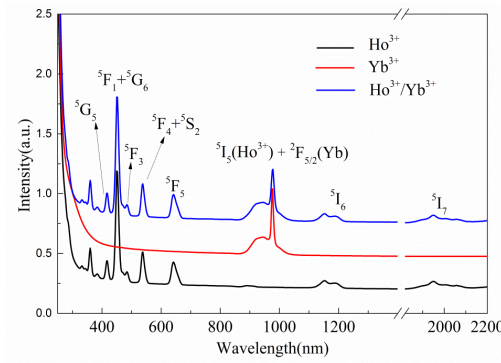


Fig. 3. Absorption spectra of Ho^{3+} singly doped, Yb^{3+} singly doped and $\text{Ho}^{3+}/\text{Yb}^{3+}$ codoped germanate glass.

3.4. Fluorescence spectra and measured lifetime at $2.0 \mu\text{m}$

Figure 4 displays the $2 \mu\text{m}$ emission spectra of $\text{Ho}^{3+}/\text{Yb}^{3+}$ codoped germanate glass doped with various Ho^{3+} concentrations excited at 980 nm LD. It is worth noting that the emission band centered at $2 \mu\text{m}$ owing to $\text{Ho}^{3+}: ^5\text{I}_7 \rightarrow ^5\text{I}_8$ transition is fairly broad. It is found that $2.0 \mu\text{m}$ fluorescence intensity firstly increases with the increment of Ho^{3+} concentration and then reduces with further increasing Ho^{3+} ions due to the concentration quenching. The optimal mid-infrared emission intensity can be obtained when Ho^{3+} concentration reaches to $0.17 \text{ mol}\%$. Hence, the optimal $2.0 \mu\text{m}$ fluorescence spectra are selected to calculate full width at half maximum (FWHM) and emission cross sections in order to estimate the gain property in this wavelength region. The optimal full width at half maximum (FWHM) is calculated to be as high as 171 nm , which is comparable to the value of $\text{Bi}_2\text{O}_3\text{-GeO}_2\text{-ZnO}$ glass that has the evident advantage in $2 \mu\text{m}$ broad-band emission [25]. Wider emission band might have potential application in mid-infrared fiber amplifier.

The emission cross-section were subsequently calculated by the following Fuchtbauer-Ladenburg equation [24]

$$\sigma_{em} = \frac{\lambda^4 A_{rad}}{8\pi cn^2} \times \frac{\lambda I(\lambda)}{\int \lambda I(\lambda) d\lambda} \quad (4)$$

where λ is the wavelength. A_{rad} is the spontaneous transition probability. $\lambda I(\lambda)$ is the emission spectrum, and n and c are the refractive index and light speed in value, respectively. The maximum dimensions was $4.9 \times 10^{-21} \text{ cm}^2$ at $2 \mu\text{m}$ as shown in the inset in Fig. 4, which is larger than that for fluoride glass ($2.47 \times 10^{-21} \text{ cm}^2$) [26] and germanate glass ($3.13 \times 10^{-21} \text{ cm}^2$) [27].

Figure 5 shows the fitting curve of the 2 μm emission (Ho^3+^5I_7 level) in the sample of optimal Ho^{3+} concentration ($x = 0.17$). The measured lifetime of the 2 μm emission (Ho^3+^5I_7 level) in the sample is 7.68 ms, which is more than 4 times and 20 times longer than the value of tellurite glass(1.6 ms) [28] and germanate glass(0.36 ms) [24], respectively. Moreover, quantum efficiency η ($\tau_m \times A_{\text{rad}}$) is another factor to evaluate the potentiality of laser material. It is worth noting that the η of $x = 0.17$ sample (79.4%) is apparent larger than fluorophosphates glass (50.64%) [29] and larger than LaF_3 glass ceramic (64.59%) [30].

Since multiphonon relaxation rate has a substantial impact on 2 μm emission, a low nonradiative decay rate is required to achieve strong 2 μm fluorescence. The multiphonon relaxation rate constant (k_{mp}) from a given excited state can be estimated from the energy-gap law [31]. The multiphonon relaxation rate constant (k_{mp}) (0.18 s^{-1}) can be calculated by [31], which demonstrated the prepared glass has a low nonradiative decay rate.

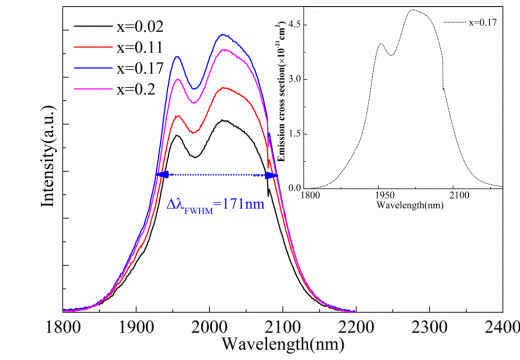


Fig. 4. 2 μm fluorescence spectra of $\text{Ho}^{3+}/\text{Yb}^{3+}$ codoped germanate glasses pumped by 980 nm LD and emission cross section of $x = 0.17$ sample (inset).

3.5 Energy transfer mechanism

The energy level diagram and energy transfer map of $\text{Ho}^{3+}/\text{Yb}^{3+}$ are presented in Fig. 6(a). The excited Yb^{3+} ions transfer pump energy to the nearby Ho^{3+} ions in ground state via the ET process, thereby exciting them to the $\text{Ho}^{3+}^5\text{I}_6$ metastable state. Then, the ions in $^5\text{I}_6$ level decay non-radiatively to $^5\text{I}_7$ level. Finally, 2 μm emissions take place due to $^5\text{I}_7 \rightarrow ^5\text{I}_8$ transition. It is worth mentioning that the residual OH^- in glass can deplete the 2 μm emission via two OH^- ions as depicted in Fig. 6(a). To better know the energy transfer process between Yb^{3+} and Ho^{3+} ions, the rate equation has been applied based on the previous studies [24, 32]. The rate equations are needed to describe this model are:

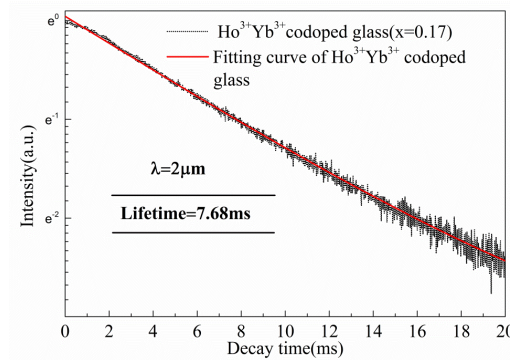


Fig. 5. The 2 μm emission lifetime curve of prepared sample ($x = 0.17$).

$$\frac{dn_1}{dt} = \frac{n_3}{\tau_3} + \frac{n_2}{\tau_2} \quad (5)$$

$$\frac{dn_2}{dt} = W_{32}n_3 - \frac{n_2}{\tau_2} \quad (6)$$

$$\frac{dn_3}{dt} = C_{D3}n_Dn_1 - \frac{n_3}{\tau_3} - W_{32}n_3 \quad (7)$$

$$\frac{dn_D}{dt} = Rn_{D0} - C_{D3}n_Dn_1 - \frac{n_D}{\tau_D} \quad (8)$$

$$\frac{dn_{D0}}{dt} = -Rn_{D0} + \frac{n_D}{\tau_D} \quad (9)$$

$$n_{D0} + n_D = n_{yb} \quad (10)$$

$$n_1 + n_2 + n_3 = n_{H_0} \quad (11)$$

where R is the pumping rate, n_{D0} and n_D are the ground state and $^2F_{5/2}$ level (Yb^{3+}) populations of donor ions, respectively. In addition, n_1 , n_2 and n_3 are the ground state, 5I_7 and 5I_6 level (Ho^{3+}) populations of acceptor ions, respectively. The transition rates between the levels i and j of a single ion are denoted by W_{ij} and the transfer rates between the donor ion and the i th level of the acceptor ion are denoted by C_{Di} . The lifetime of level i in the absence of ion-ion transfer is denoted by τ_i . In writing these equations, several approximations have been made. Excited state absorption process and the quenching effect of OH^- are neglected. Equation (12) can be obtained from these Eqs. (5)–(11) as follow:

$$n_D(t) = n_{D(0)} \exp(-(C_{D3} n_{H0} + \tau_D^{-1})t) \quad (12)$$

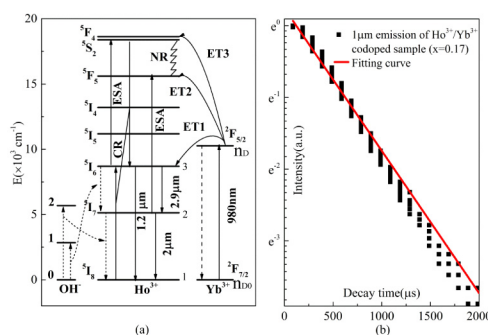


Fig. 6. (a) Energy level diagram and energy transfer map pumped by 980 nm LD in $\text{Ho}^{3+}/\text{Yb}^{3+}$ activated germanate glass. (b) The 1 μm emission lifetime curve of prepared sample ($x = 0.17$).

The lifetime of $1\mu\text{m}$ emission τ_D ($\text{Yb}^{3+}:^2\text{F}_{5/2}$ level) in prepared samples have been measured that are listed in the Table 1 to obtain values of energy transfer coefficients through exponential curve fitting of Eq. (12) as shown in Fig. 6(b). The energy transfer coefficient $C_{D3}(\text{Yb}^{3+}:^2\text{F}_{5/2} \rightarrow \text{Ho}^{3+}:^5\text{I}_6)$ of prepared samples are tabulated in Table 1. It is found that the lifetime of $^2\text{F}_{5/2}$ level keep declining with the increment of Ho^{3+} concentration, and energy transfer coefficient C_{D3} keep increasing at the same time. It can be illustrated that with the Ho^{3+} concentration increasing, Yb^{3+} ions transfer more energy to Ho^{3+} ions. It is consistent with the tendency fluorescence intensity before fluorescence quenching. On the other hand, to

some extent, it is suspected that the decrease of energy from Yb³⁺ ions to Ho³⁺ ions is due to the fluorescence quenching in prepared samples.

Table 1. The lifetime of 1 μm emission and energy transfer coefficient in prepared samples.

Sample	$\tau_D(\text{ms})$	$C_{D3}(\times 10^{-18}\text{cm}^3/\text{s})$
X = 0.02	0.9	4.99
X = 0.11	0.6	8.49
X = 0.17	0.5	16
X = 0.20	0.3	18

4. Conclusion

Ho³⁺/Yb³⁺-codoped germanate glasses with good thermal stability and high mid-infrared transmittance were successfully prepared. The prepared germanate glasses possess large spontaneous transition probability (103.38 s^{-1}) along with high emission cross section ($4.9 \times 10^{-21}\text{ cm}^2$) corresponding to the Ho³⁺:⁵I₆ \rightarrow ⁵I₇ transition. In addition, the measured lifetime of Ho³⁺:⁵I₇ level is as high as 7.68 ms, and the quantum efficiency at 2 μm can reach 79.4%. Moreover, the energy transfer processes of ²F_{5/2} level (Yb³⁺) and ⁵I₆ level (Ho³⁺) were quantitatively analyzed according to rate equation. Results indicate that the prepared germanate glass is a promising candidate for 2 μm mid-infrared laser materials applications.

Acknowledgments

This research was financially supported by the Chinese National Natural Science Foundation (No.51172252, 51372235, 61308090 and 51272243), Zhejiang Provincial Natural Science Foundation of China (No.LR14E020003, LY13F050003 and LY14E020007).